Pol. J. Environ. Stud. Vol. 32, No. 2 (2023), 1735-1742
DOI: *10.15244/pjoes/159078* ONLINE PUBLICATION DATE: 2023-02-13

Original Research

A Study of an n-TiO_2 Coated QCM Sensor's Response and Reversibility under CO_2 Exposure

Laili Mardiana[1,2], Arinto Yudi Ponco Wardoyo[1]*, Masruroh[1], Hari Arief Dharmawan[1]

[1]Physics Department, Brawijaya University, Jl. Veteran 65145, Malang, East Java, Indonesia
[2]Physics Study Program, Mataram University, Jl. Majapahit 62 Mataram, West Nusa Tenggara, Indonesia

Received: 9 November 2022
Accepted: 1 January 2023

Abstract

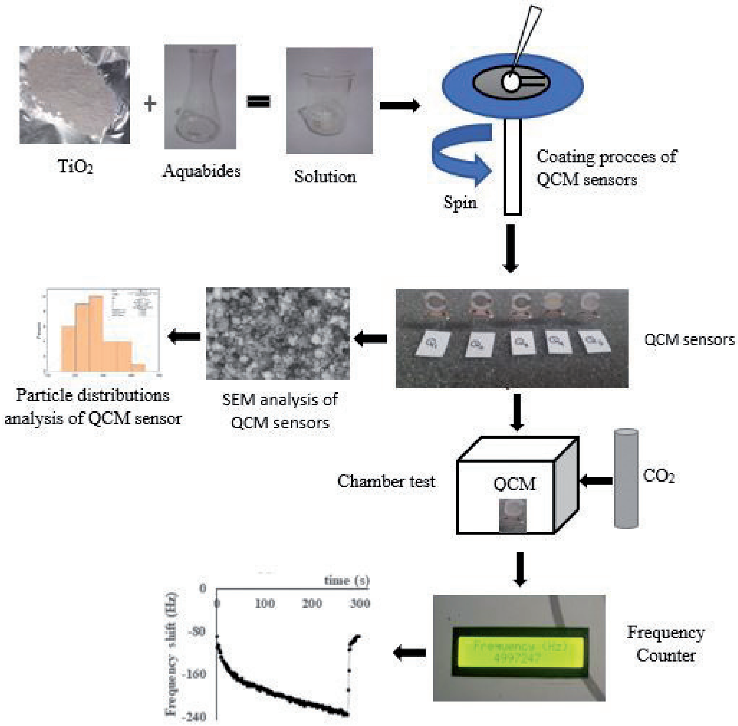

Carbon dioxide, or CO_2 gas, is an important atmospheric gas in the environment. An increase in CO_2 concentration affects environmental damage. On the other side, CO_2 concentration increases from year to year. In line with this, there is a need to develop a measurement system of CO_2 concentration with good performance. Thus, this study aims to develop a quartz crystal microbalance (QCM)-based

*e-mail: a.wardoyo@ub.ac.id

CO_2 sensor using titanium dioxide nanoparticles and to identify the response and reversibility levels. For this purpose, this study used five sensors with different thicknesses: Q_1, Q_2, Q_3, Q_4, and Q_5 to identify the response and reversibility responses. The results show that the sensors had a frequency shift of 5.14 kHz (Q_1), 5.19 kHz (Q_2), 5.70 kHz (Q_3), 5.78 kHz (Q_4), and 6.05 kHz (Q_5). The response times are 80.1 s (Q_1), 82.8 s (Q_2), 84.6 s (Q_3), 85.5 s (Q_4), and 247.5 s (Q_5). The frequency shifts and the response times indicate that Q_5 has the best response for CO_2. All sensors have fast recovery times, 10.8 s to 21.6 s. It can be concluded that the developed sensors have good response times, recovery times, and reversibility levels for CO_2 gas detection. This sensor can be used as an alternative to a CO_2 gas concentration measurement system, providing a novel and rapid detection method and fast recovery time.

Keywords: carbon dioxide, measurement, quartz crystal microbalance, sensor, titanium dioxide

Introduction

Carbon dioxide (CO_2) gas is one of the air pollutants related to environmental quality. This gas is emitted from many sources and is widely mitigated in many countries regarding air quality [1]. This gas plays an important role in many sectors, such as air quality, farm, food quality, greenhouse, and human life [2-4]. CO_2 gas concentration in the atmosphere is <400 ppm [5] and keeps increasing with a gradient of 2 ppm/year. A previous study predicts that CO_2 concentrations will reach 500 ppm to 1,000 ppm in 2100 [6]. This condition may influence and disturb the environment and health, including humans, animals, and plants. These distractions indicate the need for CO_2 gas mitigation, including continuous and comprehensive measurement and monitoring systems.

CO_2 gas concentration can be measured using many methods, such as a non-dispersive infrared (NDIR) sensor [7], a Piezoresistive Micro-Electro-Mechanical Systems (MEMS) [8], highly-sensitive MEMS microphones [9], and quartz crystal microbalance (QCM) sensor [5, 10-14]. Especially for QCM, this gravimetric sensor has high precision, high sensitivity to mass, a low power mode, and compactness [12, 13]. QCM is a mass sensor that detects a mass change on a nanogram scale. This sensor is very suitable for detecting target gasses based on the piezoelectric principle [4]. There will be a frequency shift when a certain analyte deposits onto the QCM's surface [14]. For performance increase purposes, a sensitive layer is applied to its surface using many materials, such as polymer, metal oxide, and other functional films [10-16]. For example, ZnO film was applied as the sensitive layer for ethanol gas detection [17]. Other applications are SnO_2 NFs/PDA for formaldehyde gas detection [18] and polyvinyl acetate (PVAc) film for VOC (Volatile Organic Compounds) detection (benzene, toluene, and xylene or BTX) [19].

Titanium dioxide, or TiO_2, is one of the most popular materials for the sensing layer. This material has three phases: rutile, anatase, and brookite [20-22]. Especially for the anatase phase, this phase has good chemical stability [23]. Physically, this material has good sensitivity, high tolerance to temperature, low cost, and high stability [24-29].

Development of a CO_2 sensor based on TiO_2 coated-QCM has been conducted [30, 31]. The previous studies show that the sensors adsorbed CO_2 gas with low recovery time and reversibility. Thus, there is a need to increase the sensor's performance since the sensor quality depends on the crystal structure, particle size distribution, layer thicknesses, and layer morphology [23, 31]. In line with this, this study focuses on modifying a QCM surface to increase the sensor performance by using an anatase phase-TiO_2 film as the sensitive layer. This study identifies the best response time, recovery time, and reversibility level by modifying the variated thicknesses of an anatase phase-TiO_2. This study may contribute to the CO_2 gas concentration measurement system with a better performance.

Materials and Methods

Gas Sample

CO_2 gas was purchased from P.T. Malson Gas Surabaya (purity = 99.98%, volume = 5 L).

Sensor Preparation

This study used five QCM sensors (Q_1, Q_2, Q_3, Q_4, and Q_5) with a fundamental frequency (f_o) of 4.999265 MHz (silver electrodes). These QCMs were coated with TiO_2 nanoparticles (sigma Aldrich 99%, anatase phase). The nanoparticles were deposited on the QCM surface with five different concentrations: 0.5 µL (Q_1), 1 µL (Q_2), 3 µL (Q_3), 3.5 µL (Q_4), and 5 µL (Q_5) using a spin coating method. The spin coating process was conducted twice per sensor with different rotation speeds: 300 rpm (for 10 s) and then 2500 rpm (for 60 s) [32]. The prepared sensors were observed under scanning electron microscopy (JEOL-JCM7000). The diameters of the particle distribution were analyzed using Image-J software.

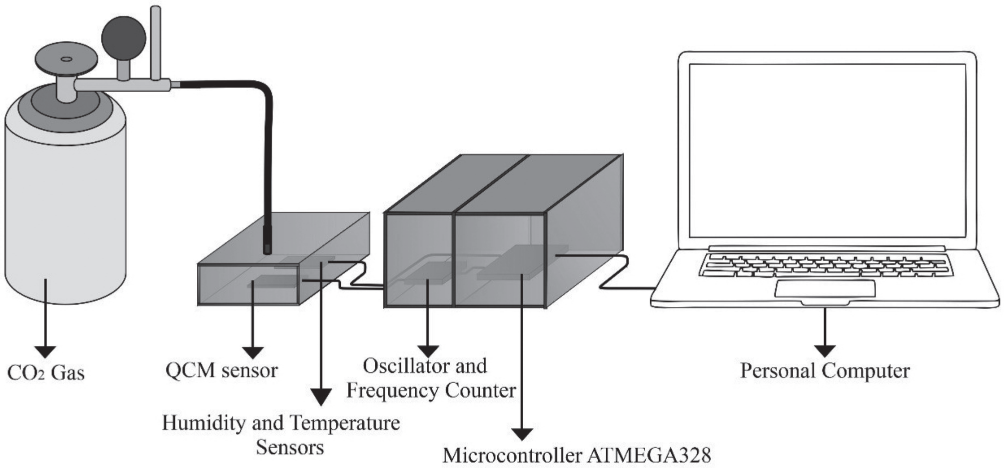

Fig. 1. Experimental setup for the exposure and measurement.

Measurement System

The measurement was conducted using an oscillator, a microcontroller, a gas flow control, and a sensor box (Fig. 1). The oscillator was used to drive and trigger the oscillation frequency before and after gas exposure. The oscillator was connected to the microcontroller (Atmega 328) as the frequency (f) counter. The gas flow control consisted of a cylinder, a tube (diameter = 0.4 cm), a valve, and a regulator. The sensors were installed inside the sensor box (vacuum condition).

Measurement Setup

Fig. 1 interprets the measurement setup. Each sensor was exposed to the gas sample (flow rate = 1 L/minute) until the sensor reached a steady condition. The frequency shift (Δf) was measured with an interval of 1 s using the equation below.

$$\Delta f = f - f_o \quad (1)$$

The response and recovery time were determined based on the full-scale reading and full-scale recovery reading [18, 33]. The reversibility was determined by analyzing the resulting curve, where the reversibility was good if the measured frequency returned to its initial frequency [15].

Results

Sensor Morphology Observation

Fig. 2 shows the morphological image of the deposited TiO_2 on the surface of QCM. Based on the initial frequency test, these deposition processes caused each sensor to have different frequency shifts: 5.14 kHz (Q_1), 5.19 kHz (Q_2), 5.70 kHz (Q_3), 5.78 kHz (Q_4), and 6.05 kHz (Q_5). These results confirm that the TiO_2 layer has been successfully deposited on the sensor's surface. According to the SEM images in Fig. 2, it can be seen that each sensor has a different morphological form, including the particle size and the microstructure of each sample. The spherical-shaped TiO_2 particles are clearly shown in the nanoscale range.

Fig. 2e) shows that the most uniform surface was obtained in Q_5. At the same time, the lowest one is referred to as Q_1 (Fig. 2a). The digital image processing results indeed support that Q_5 has the smallest particle size distribution among all sensors. Based on Fig. 2(a-c), the particle size distribution of Q_1, $Q_{2,}$ and Q_3 are 393.26±22.57 nm, 333.35±9.21 nm, and 322.77±23.93 nm, respectively. Q_4, which has the medium layer, has 374.02±5.53 nm (Fig. 2d). The last sensor, Q_5, has a particle size distribution of 258.23±24.81 nm, determined as the smallest particle size distribution. A smaller particle diameter, a bigger surface volume fraction [34]. A bigger volume fraction may increase the particle binding. In line with this, Q_5 has the highest volume fraction and potential as the CO_2 sensing device. As a mass-type CO_2 gas sensor, the physical parameters have important roles in its performance, including pore volume, surface area, physical adsorption, and pore size. Thus, as shown in this digital image processing, the gas sensing properties may be influenced by the pore size distribution, including the adsorption–desorption factors.

Sensor Responses under CO_2 Exposure

Figs 3-4 shows the sensors' frequency shift, response time, and recovery time after exposure to the sample gas. All sensors have different response times (t_{on}) and recovery times (t_{off}), indicating the CO_2 gas adsorption ability. The response times are 80.1 s, 82.8 s, 84.6 s, 85.5 s, and 247.5 s, respectively, for Q_1, Q_2, Q_3, Q_4, and Q_5. The recovery times for Q_1 – Q_5 are 10.8 s, 10.8 s, 11.7 s, 12.6 s, and 21.6 s, consecutively. According to these results, Q_1 has the least response

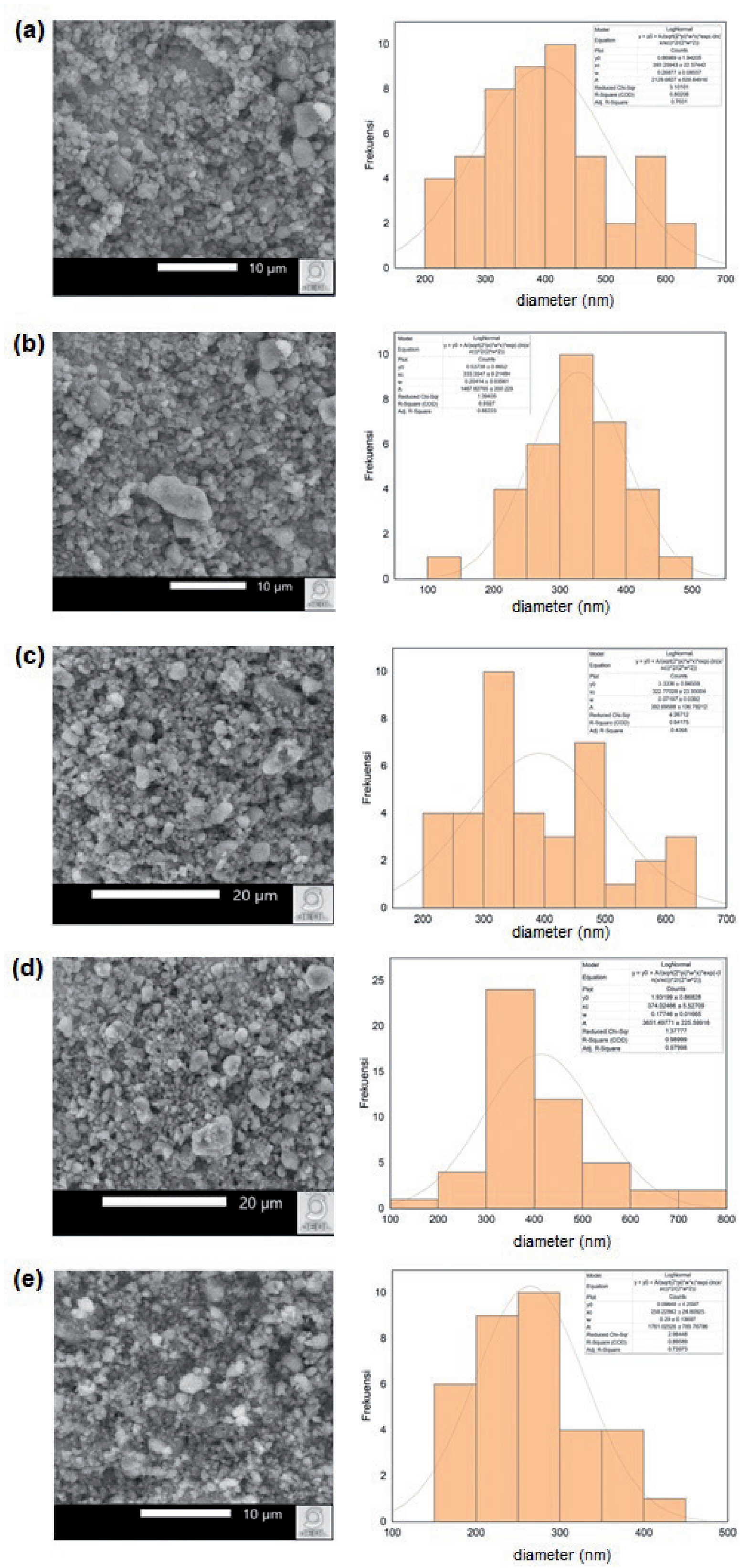

Fig. 2. Morphological images and particle size distributions of the QCM sensors: a) Q1; b) Q2; c) Q3; d) Q4; and e) Q5.

time (Fig. 4a) and recovery time (Fig. 4b) than other sensors, indicating the lowest responses. The results are related to the different thicknesses, which may influence the sensor performance.

Fig. 3 also interprets the active zone. The figure shows that Q_5 has a higher adsorption ability than Q_1 – Q_4, indicated by a longer adsorption duration. Besides, Q_3 has good reversibility compared to Q_1, Q_2,

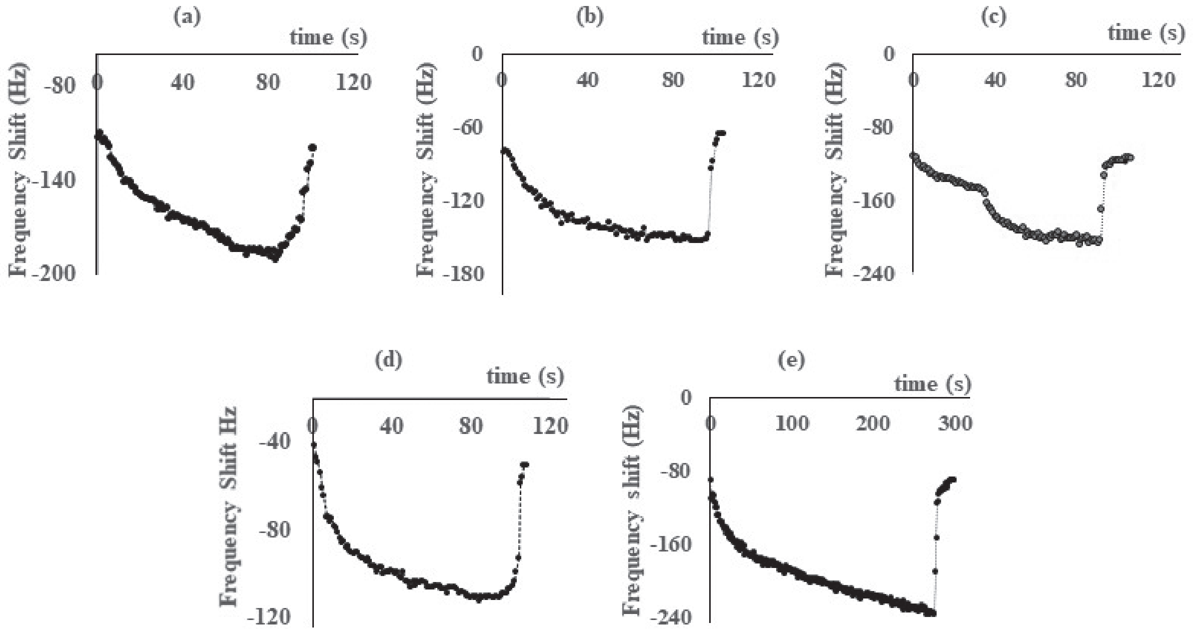

Fig. 3. Frequency responses of all sensors: a) Q1; b) Q2; c) Q3; d) Q4; and e) Q5.

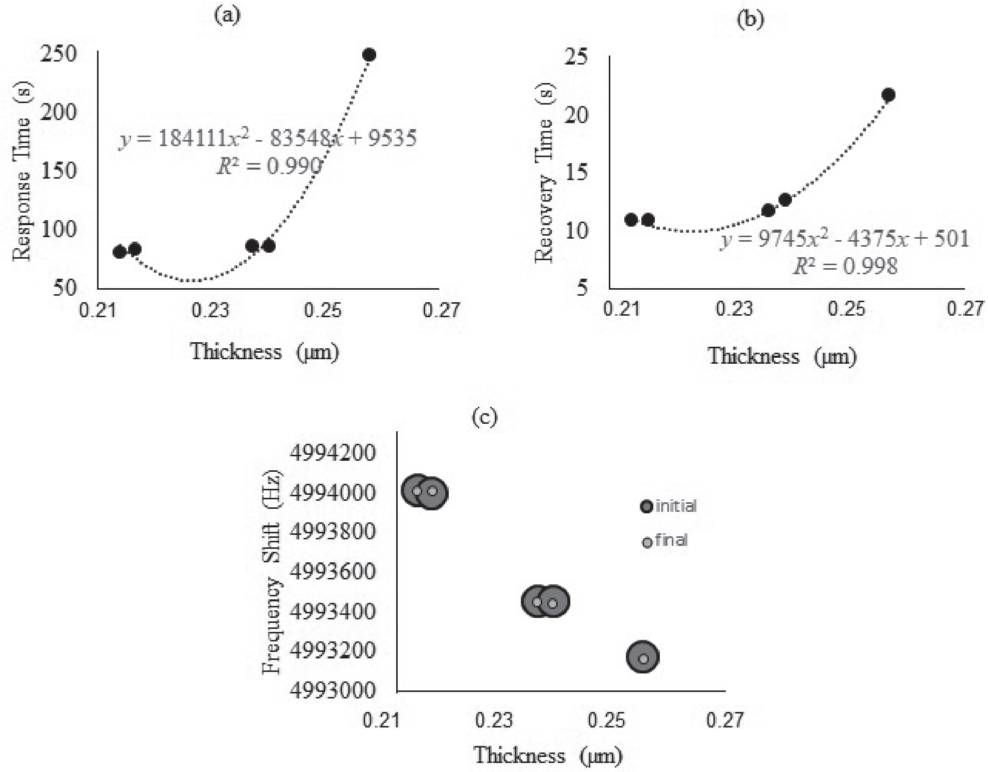

Fig. 4. Thicknesses and response – recovery times of all sensors.

Q_4 and Q_5 shown by the best frequency oscillation (the least frequency shift regarding the initial frequency) and recovery state after reaching the steady state. The recovery state can be seen from the frequency value (Fig. 4b), which returns to normal again (reaching the initial frequency, Fig. 4c).

The data indicate that all sensors work well to detect CO_2 gas concentrations. However, in terms of the response and recovery times, the most performance is obtained in Q_5. Although the best reversibility is obtained in Q_3, Q_5 has the best surface homogeneity indicating the highest flexibility and stability levels

Table 1. Sensor's performance related to different thicknesses.

Sensors	V (µL)	Respons Times (s)	Recovery Times (s)	Δf (Hz)	Reversibility Levels
Q1	0.5	80.1	10.8	7	High
Q2	1	82.2	10.8	-15	Low
Q3	3	84.6	11.7	3	High
Q4	3.5	85.5	12.6	9	High
Q5	5	247.5	21.6	7	High

(see Table 1). As the impact, Q_5 has the best adsorption capability.

Discussion

QCM is a mass sensor based on a piezoelectric principle. The frequency will decrease if a mass is deposited onto the QCM's surface [35]. This study shows that the frequency decreases when the exposed mass increases. The correlation between frequency shift and mass change (Δm) is expressed by Sauerbrey's equation:

$$\Delta f = -C_f . \Delta m \quad (2)$$

The frequency change or frequency shift is denoted by Δf. C_f represents the sensor sensitivity calculated from:

$$C_f = \frac{2.n.{f_0}^2}{(\mu_q \rho_q)^{1/2}} \quad (3)$$

The modulus shear is μ_q, 2.947 x 10^{11} g/cm s^2), ρ_q is the quartz density (2.648 g/cm^3), and n is the harmonic number when the crystal is driven.

The preliminary study shows that a bare QCM sensor has lesser responses among all similar gas exposures. The bare QCM sensors exhibit lower frequency shifts than the TiO_2 coated-QCM. In other words, a bare QCM (uncoated QCM) has no significant differences between each treatment related to the mass loading effect. No specific loaded and unloaded mass can be analyzed due to the absence of the selective material or layer.

As expected, the addition of sensitive materials on the surface of the QCM sensor may influence the frequency responses. As obtained in this study, the coated QCM sensor has a good performance in terms of frequency shift. The deposited sensitive film determines the sensor selectivity, whether an immune sensor [36], a bioaerosol sensor [37], or a gas sensor [38, 39]. That is why the sensitive layer determines the performance, such as the used TiO_2. TiO_2 is a type-n semiconductor with three activation energies: 3.2 eV, 3.02, and 2.9 eV [40, 41]. These energies influence the interaction between the layer and the target gas.

The adsorption process is related to the CO_2 gas as an oxidizing gas. CO_2 has a linear bonded atom with a stable structure. As conducted in this study, the anatase phase TiO_2 has three different TiO_2 percentages and thicknesses that may influence the adsorption ability. This process is influenced by the physisorption and chemisorption systems and the activation energy. Oxygen molecules are adsorped when the sensor is coated by n-TiO_2 and exposed to CO_2 gas. The bounding is referred to as a Van der Waals bonding mechanism [23, 24]. That is why the Q_5 sensor has the best ability to adsorb CO_2 gas. This sensor also has a rigid and uniform morphology [15]. Q_1 – Q_4 have less-uniform surfaces that influence their performances and rigidities, resulting in low reversibility. A higher oscillation frequency indicates these results compared to their initial frequencies. The probable parameter that causes this result is the decrease of TiO_2 mass after exposure. Using a sensitivity approach, it can be found that a bare sensor only has a sensitivity of 17.7 ng/Hz. Then, for example, the Q_2 sensor loses 265 ng of mass.

The different results are also influenced by the different morphologies and thicknesses (Fig. 4a-c), resulting in different characteristics (response – recovery times). The thicknesses of the analyte and film on the sensor surface are related to the adsorption duration [18]. According to the Langmuir adsorption:

$$\Delta m_t = \Delta m_\infty \left(1 - e^{\frac{t}{\tau}}\right) \quad (4)$$

The maximum amount of CO_2 molecule on the sensor surface is denoted by Δm_∞, for the time $t \rightarrow \infty$. Time t is the relaxation time, while time τ is the response time [15].

Conclusions

The n-TiO_2 coated-QCM sensor can adsorb CO_2 gas. The differences between crystal phase, particle diameter, n-TiO_2, and thickness change the QCM characteristics. It can be seen from the response time (80.1 s to 247.5 s) and recovery time (10.8 s to 21.6 s). The best stability and flexibility levels are obtained from the Q_5 sensor due to its uniform and rigid surface, resulting in the best CO_2 adsorption ability.

Among all sensors, Q_5 indeed has the best performance. The prepared sensors work well to detect CO_2 gas in a certain concentration. As a preliminary study, further research should be conducted to identify the range limit of the gas concentration. Sensor optimation should be carried out in the laboratory and the real condition testing. For a real application, such layers with modified surface structures may be of interest for studying sensor optimation.

Acknowledgments

All authors wish to thank Mataram University for part of the funding. The authors also thank Brawijaya University for its experimental facilities.

Conflict of Interest

The authors declare no conflict of interest.

References

1. GALVAN L.P.C., BHATTI U.A., CAMPO C.C., TRUJILLO R.A.S. The nexus between CO_2 emission, economic growth, trade openness: Evidences from middle-income trap countries. Frontiers in Environmental Sciences **10**, 1, **2022**.
2. BAGHERI F., HARATIZADEH H. UV-activated CO_2 sensor based on ZnO nanoparticles at low temperatures. Materials Science in Semiconductor Processing **141**, 106422, **2022**.
3. KAROUEI S.F.H., MOGHADDAM H.M. P-p heterojunction of polymer/hierarchical mesoporous $LaFeO_3$ microsphere as CO_2 gas sensing under high humidity. Applied Surface Science **479**, 1029, **2019**.
4. BEROUAKEN M., TALBI L., ALKAMA R., SAM S., MENARI H., CHEBOUT K., MANSERI A., BOUCHEHAM A., GABOUZE N. Quartz crystal microbalance coated with vanadium oxide thin film for CO_2 gas sensor at room temperature. Arabian Journal for Science and Engineering **43** (11), 5957, **2018**.
5. KHAN R.R.M., SALEEM R., BASHIR R., PERVAIZ M., NAZ S., REHMAN S.U., YOUNAS U., BATOOL S.E., HAIDER H.M.F., IQBAL M., ADNAN A. Highly selective and efficient porous Cu-Sn bimetallic electrocatalyst for CO_2 reduction to formate. Polish Journal of Environmental Studies **30** (5), 4579, **2021**.
6. NG C.W.W., TASNIM R., COO J.L. Effects of atmospheric CO_2 concentration on soil-water retention and induced suction in vegetated soil. Engineering Geology **242**, 108, **2018**.
7. ISHIHARA H., MASUNO K., ISHII M., KUMAGAI S., SASAKI M. Enhanced plasmonic wavelength selective infrared emission combined with microheater**.** Materials **10**, 1085, **2017**.
8. JULIET V., VIVIN S. Peizoresistive mems cantilever based CO_2 gas sensor. International Journal of Computer Applications, **49** (18), 0975, **2012**.
9. POPA D., UDREA F. Towards integrated mid-infrared gas sensors. Sensors **19**, 2076, **2019**.
10. SARANGO L., BENITO J., GASCÓN I., ZORNOZA B., CORONAS J. Homogeneous thin coatings of zeolitic imidazolate frameworks prepared on quartz crystal sensors for CO_2 adsorption. Microporous and Mesoporous Materials **272**, 44, **2018**.
11. ANDRÉS M.A., BENZAQUI M., SERRE C., STEUNOU N., GASCÓN I. Fabrication of ultrathin MIL-96 (Al) films and study of CO_2 adsorption/desorption processes using Quartz Crystal Microbalance. Journal of Colloid and Interface Science **519**, 88, **2018**.
12. ALEV O., OZDEMIR O., GOLDENBERG E., ARSLAN, C.L., BÜYÜKK¨OSE S., OZTÜRK Z.Z. WS_2 thin film based quartz crystal microbalance gas sensor for dimethyl methylphosphonate detection at room temperature. Thin Solid Films Journal **45**, 2, **2022**.
13. LIU X., WANG J., HOU J. Repeatability and sensitivity of quartz crystal microbalance (QCM) sensor array modified with four sensitive materials. Materials Science in Semiconductor Processing **147**, 106764, **2022**.
14. MURAOKA S., KIYOHARA Y., OUE H., HIGASHIMOTO S. A CO_2 sensor using a quartz crystal microbalance coated with a sensitive membrane. Electronics and Communications in Japan **97** (2), 60, **2014**.
15. FAUZI F., RIANJANU A. SANTOSO I., TRIYANA K. Physical gas and humidity sensing with quartz crystal microbalance (QCM) coated with graphene-based materials – A mini review. Sensors & Actuators: A. Physical **330**, 112837, **2021**.
16. NUGROHO D.B., RIANJANU A., TRIYANA K., KUSUMAATMAJA A., ROTO R. Quartz crystal microbalance-coated cellulose acetate nanofibers overlaid with chitosan for detection of acetic anhydride vapor. Results in Physics Journal **15**, 102680, **2019**.
17. ITO T., FUJII Y., YAMANISHI N., ASAI N., SHIMIZU T., SHINGUBARA S. Electrodeposited ZnO thin film on twin sensor QCM for Sensing of ethanol at room temperature. Procedia Engineering **168**, 411, **2016**.
18. WANG L., GAO J., XU J. Chemical QCM formaldehyde sensing materials: Design and sensing mechanism. Sensors & Actuators: B. Chemical **293**, 71, **2019.**
19. RIANJANU A., HASANAH S.A., NUGROHO D.B., KUSUMAATMAJA A., ROTO R., TRIYANA K. Polyvinyl acetate film-based quartz crystal microbalance for the detection of benzene, toluene, and xylene vapors in air. Chemosensors **7**, 20, **2019**.
20. GOMES M.T.S.R., NOGUEIRA P.S.T., OLIVEIRA J.A.B.P. Quantification of CO_2, SO_2, NH_3, and H_2S with a single coated piezoelectric quartz crystal. Sensors and Actuators, B: Chemical **68** (1), 218, **2000**.
21. ADDABBO T., FORT A., MUGNAINI M., VIGNOLI V., BALDI A., BRUZZI M. Quartz-crystal microbalance gas sensors based on TiO_2 nanoparticles. IEEE Transactions on Instrumentation and Measurement **67** (3), 722, **2018**.
22. CHEN X., SELLONI A. Introduction: Titanium dioxide (TiO_2) nanomaterials. Chemical Reviews **114** (19), 9281, **2014**.
23. CHACHULI S.A.M., HAMIDON M.N., MAMAT M.S., ERTUGRUL M., ABDULLAH N.H. A hydrogen gas sensor based on TiO_2 nanoparticles on alumina substrate. Sensors **18** (8), 1, **2018**.
24. NISAR J., TOPALIAN Z., SARKAR A.D., OSTERLUND L., AHUJA R. TiO_2 based gas sensor: a possible application to SO_2. ACS Applied Materials and Interfaces **5** (17), 8516, **2013**.
25. RAZA M.A., HABIB A., KANWAL Z., HUSSAIN S.S., IQBAL M.J., SALEEM M., RIAZ S., NASEEM S. Optical

CO_2 gas sensing based on TiO_2 thin films of diverse thickness decorated with silver nanoparticles. Advances in Materials Science and Engineering **2018**, 1, **2018**.
26. BAI J., ZHOU B. Titanium dioxide nanomaterials for sensor applications. Chemical Reviews **114** (19), 10131, **2014**.
27. BOYADJIEV S., GEORGIEVA V., VERGOV L., SZILÁGYI I.M. QCM gas sensor characterization of ALD-grown very thin TiO_2 films. Journal of Physics: Conference Series **992** (1), 1, **2018**.
28. BOYADZHIEV S., GEORGIEVA V., RASSOVSKA M. Characterization of reactive sputtered TiO_2 thin films for gas sensor applications. Journal of Physics: Conference Series **253** (1), 1, **2010**.
29. ZAKRZEWSKA K., RADECKA M. TiO_2-based nanomaterials for gas sensing- influence of anatase and rutile contributions. Nanoscale Research Letters, **12** (1), 1, **2017**.
30. MARDIANA L., WARDOYO A.Y.P., MASRUROH M., DHARMAWAN H.A. Synthesis TiO_2 using sonochemical method and responses the CO_2 gas of the nanoparticle TiO_2 layers on the QCM sensor surfaces. Journal of Physics: Conference Series **2165** (1), 1, **2022**.
31. GHOLAMI M., BAHAR M. The preparation of TiO_2 nanoparticles and investigation of its electrical properties as CO_2 gas sensor at room temperature. Chemical Physics Letter **48** (2), 9626, **2012**.
32. ADDABBO T., FORT A., MUGNAINI M., TANI M., VIGNOLI V., BRUZZI M. Quartz crystal microbalance sensors based on TiO_2 nanoparticles for gas sensing. IEEE Xplore 1, **2017**.
33. RAHAYU E.I.P., PUTRI N.P. The effect of solution concentration and deposition time on viscoelasticity and morphology of polyaniline coating. Journal of Physics: Conference Series **1491**, 1, **2020**.
34. YUWONO A.S., LAMMERS P.S. Performance test of a sensor array-based odor detection instrument. Journal of Science and Research Development **3**, 9, **2004**.
35. VINH N. T., DANG T. V., HANG B. T., LE A., TUAN N. T., VINH L. K. Effect of ferric ion [Fe^{3+}] and [Fe^{2+}] on SO_2 adsorption ability of γ-Fe_2O_3 nanoparticles for mass-type gas sensors. Sensors Actuators A Phys., **331**, 112981, **2021**.
36. BRAGAZZI N.L., AMICIZIA D., PANATTO D., TRAMALLONI D., VALLE I., GASPARINI R. Quartz-crystal microbalance (QCM) for public health: an overview of its applications. Advances in Protein Chemistry and Structural Biology **101**, 149, **2015**.
37. YOON J., SUK S. Talanta Quartz crystal microbalance cardiac Troponin I immunosensors employing signal amplification with TiO_2 nanoparticle photocatalyst. Talanta **228**, 122233. **2021**.
38. BUDIANTO A., WARDOYO A.Y.P., MASRUROH M., DHARMAWAN H.A. An airborne fungal spore mass measurement system based on graphene oxide coated QCM. Polish Journal of Environmental Studies **31** (4), 3523, **2022**.
39. WANG L. Metal-organic frameworks for QCM-based gas sensors: A review. Sensors and Actuators A: Physical **307**, 111984, **2020**.
40. RZAIJ J.M., ABASS A.M. Review on: TiO_2 thin film as a metal oxide gas sensor. Journal of Chemical Reviews **2** (2), 114, **2020**.
41. HAIDER A.J., JAMEEL Z.N., AL-HUSSAINI I.H.M. Review on: Titanium dioxide applications. Energy Procedia **157**, 17, **2019**.